

Two-Fluid Performance Limits: Stellarator and Tokamak Compared

L.E. Sugiyama¹

H.R. Strauss², W. Park³, G.Y. Fu³

¹Massachusetts Institute of Technology, Cambridge MA 02139-4307

²New York University, New York NY 10012

³Princeton Plasma Physics Laboratory, Princeton NJ 85430

Intl. Sherwood Theory Conference
Missoula MT, April 26–28, 2004

TOPICS

- **Basic two-fluid limits on high beta performance of stellarators:**

Numerical, nonlinear, complete 3D configuration, using M3D code.

Quasi-axisymmetric stellarator NCSX and equivalent axisymmetric cases

- **Two-fluid effects stabilize MHD modes at high mode number that set the theoretically strongest limits on stellarators**

- **Two-fluid effects ($\nabla_{\parallel} p_e / en$ in Ohm's law) enhance nonlinear magnetic reconnection rates**

Stellarator beta may be limited by magnetic reconnection, not MHD modes

- **Two-fluid effects introduce important global steady state conditions in toroidal plasmas**

- **Importance of $\nabla_{\parallel} p_e$ in Ohm's law.**

Two-fluid model

- Simple nonlinear model to capture “low frequency” dynamics perpendicular to B, based on drift ordering: $v/v_{th} \sim \delta \ll 1$, $\partial/\partial t \sim \delta v_{th}/L$, $\omega/\Omega_{ci} \sim \delta \rho_i/L \sim \delta^2$ (part of M3D code, Sugiyama and Park, Phys. Plasmas (2000)).
- Parallel-to-B dynamics includes parallel thermal equilibration along B. (Neoclassical parallel stresses $\nabla \cdot \Pi_{j\parallel}$ dropped here.)

$$\frac{\partial v_i}{\partial t} + (v_i \cdot \nabla)v_i = \frac{J \times B}{nm_i} - \frac{\nabla p}{nm_i} - \frac{\nabla \cdot \Pi_i^{gv}}{nm_i} - \frac{\nabla \cdot \Pi_{i\parallel}}{nm_i} + \mu_{\perp} \nabla^2 v_i$$

$$E + v_e \times B = \eta J - \frac{\nabla p_e}{en_e} - \frac{0.71}{e} \nabla_{\parallel} T_e - \frac{\nabla \cdot \Pi_{e\parallel}}{en_e}$$

$$\frac{\partial p_i}{\partial t} + v_i \cdot \nabla p_i = -\Gamma_i p_i \nabla \cdot v_i + \nabla \cdot n_i \kappa_i \cdot \nabla \frac{p_i}{n_i}$$

$$\frac{\partial p_e}{\partial t} + v_e \cdot \nabla p_e = -\Gamma_e p_e \nabla \cdot v_e + \nabla \cdot n_e \kappa_e \cdot \nabla \frac{p_e}{n_e}$$

$$\frac{\partial n_e}{\partial t} + v_e \cdot \nabla n_e = -n_e \nabla \cdot v_e$$

$$\frac{\partial B}{\partial t} = -\nabla \times E \quad J = \nabla \times B \quad \nabla \cdot B = 0 \quad \nabla \cdot J = 0$$

- Define fluid velocities in terms of $\mathbf{v}_{*e} \equiv -\mathbf{B} \times \nabla p_e / (en_e B^2)$ as $\mathbf{v}_i = \mathbf{v} + \mathbf{v}_{di}$, $\mathbf{v}_e = \mathbf{v} + \mathbf{v}_{*e} - \mathbf{J}_{\parallel} / en_e$, where $\mathbf{v}_{di} \equiv \mathbf{J}_{\perp} / (en_e) + \mathbf{v}_{*e}$.

$$\begin{aligned}
\frac{\partial \mathbf{v}}{\partial t} + (\mathbf{v} \cdot \nabla) \mathbf{v} &= -(\mathbf{v}_{di} \cdot \nabla) \mathbf{v}_{\perp} + \frac{\mathbf{J} \times \mathbf{B}}{nm_i} - \frac{\nabla p}{nm_i} + \mu_{\perp} \nabla^2 (\mathbf{v} + \mathbf{v}_{di}) + \mathcal{V}_{gv} - \frac{\mathbf{b}\mathbf{b} \cdot \nabla \cdot \Pi_{i\parallel}}{nm_i} \\
\frac{\partial \mathbf{B}}{\partial t} &= -\nabla \times \mathbf{E}, \quad \mathbf{E} + \mathbf{v} \times \mathbf{B} = \eta \mathbf{J}^* - \frac{\nabla_{\parallel} p_e}{en} - \frac{0.71}{e} \nabla_{\parallel} T_e - \frac{\mathbf{b}\mathbf{b} \cdot \nabla \cdot \Pi_{e\parallel}}{en} \\
\frac{\partial T_i}{\partial t} + \mathbf{v} \cdot \nabla T_i &= -\hat{\Gamma} T_i \nabla \cdot \mathbf{v} + \frac{1}{n} \nabla \cdot n \kappa_i \cdot \nabla T_i - \mathbf{v}_{di} \cdot \nabla T_i - \hat{\Gamma} T_i \nabla \cdot \mathbf{v}_{di} - \frac{\Gamma}{n} \nabla \cdot (p_i \mathbf{v}_{*Ti}) \\
\frac{\partial T_e}{\partial t} + \mathbf{v} \cdot \nabla T_e &= -\hat{\Gamma} T_e \nabla \cdot \mathbf{v} + \frac{1}{n} \nabla \cdot n \kappa_e \cdot \nabla T_e - \mathbf{v}_{*e} \cdot \nabla T_e - \hat{\Gamma} T_e \nabla \cdot (\mathbf{v}_{*e} + \mathbf{v}_{\parallel e}) + \\
\frac{\partial n}{\partial t} + \mathbf{v} \cdot \nabla n &= -n \nabla \cdot (\mathbf{v} + \mathbf{v}_{*e}) + \mathbf{B} \cdot \nabla \left(\frac{\mathbf{J} \cdot \mathbf{B}}{eB^2} \right) \quad \parallel \quad \frac{\mathbf{J} \cdot \mathbf{B}}{enB^2} \mathbf{B} \cdot \nabla T_e - \frac{\Gamma}{n} \nabla \cdot (p_e \mathbf{v}_{*Te})
\end{aligned}$$

The parallel diffusion $\nabla \cdot \kappa_{j\parallel} \nabla_{\parallel} T_j$, $j = i, e$, is treated as if due to parallel wave motion with speed sv_A (artificial sound method):

$$\begin{aligned}
\partial T / \partial t &= sB / \rho \cdot \nabla v_A \\
\partial v_A / \partial t &= sB \cdot \nabla T + \nu \nabla^2 v_A.
\end{aligned}$$

Two-Fluid Parameters

- MHD steady states with $v = 0$ depend only on the combination $\eta\mu$ in addition to the equilibrium quantities. (W. Park, et al., Phys. Fluids 29 1171 (1986))
 - Scaling η to $\alpha\eta$ and μ to μ/α , changes v to αv , but leaves p , B unchanged.
- Two-fluid plasma parameters:
 - The two-fluid terms are proportional to the two-fluid parameter $H \equiv 1/\Omega_{ci}\tau_A = c/(\omega_{pi}R)$.
 - p_e/p at fixed total pressure p .
 - $\nabla_{\parallel} p_e/p_e$.
 - v_e and v_i are not both zero in steady state, in general.
- Simulation parameters
 - Resistivity (Lundquist number) $S = 10^5$
 - Ion perpendicular viscosity $\mu = 5 \times 10^{-4}$, in some cases extra toroidal viscosity
 - $H = 0.02$ (actual value)



NCSX

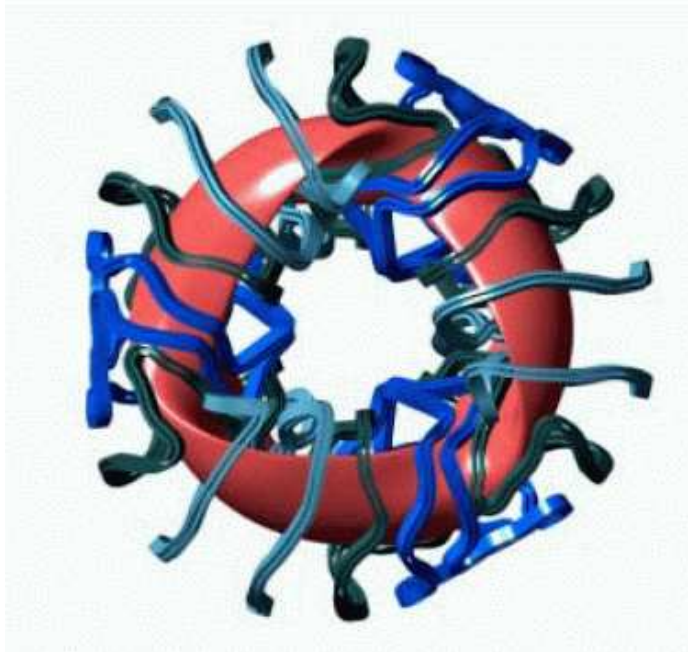
$$R = 1.4 \text{ m}$$

$$R/\langle a \rangle = 4.4$$

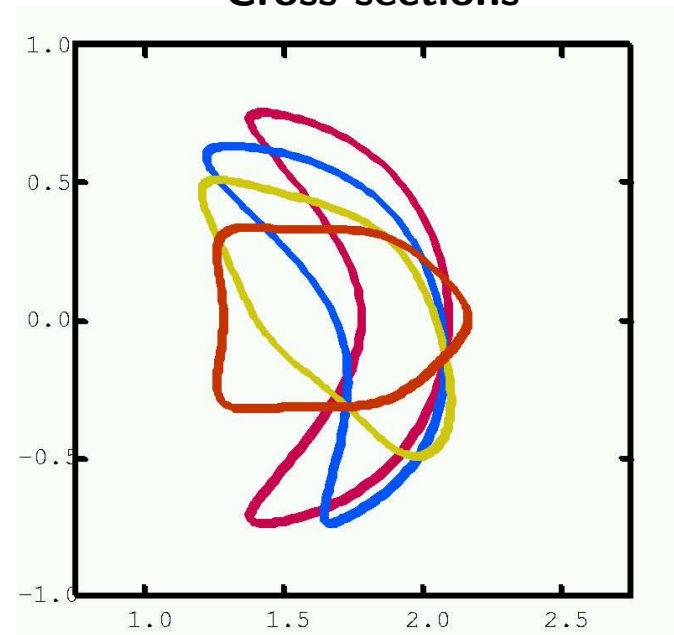
$$B_T = 1.44 \text{ T}$$

$$\nu/2\pi = 0.4\text{--}0.65$$

3 Toroidal periods

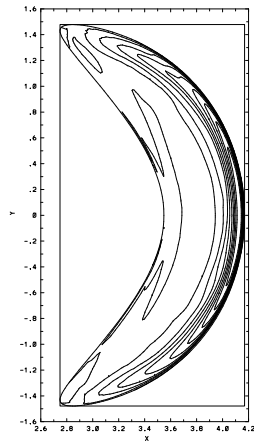


Cross sections

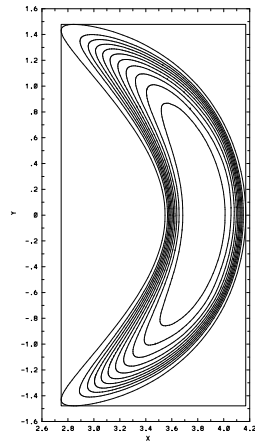


- NCSX MHD equilibrium profiles for $\beta = 7\%$.

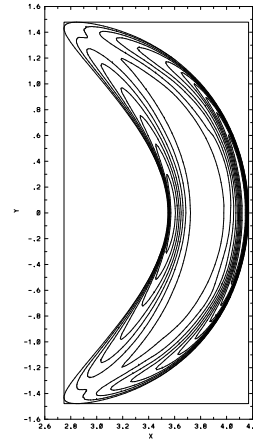
RJ_ϕ



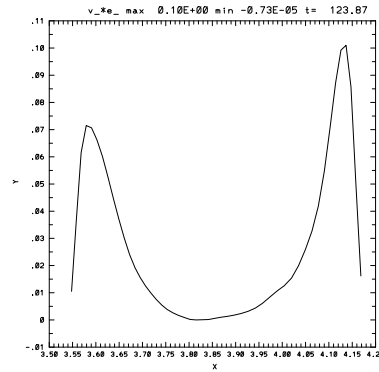
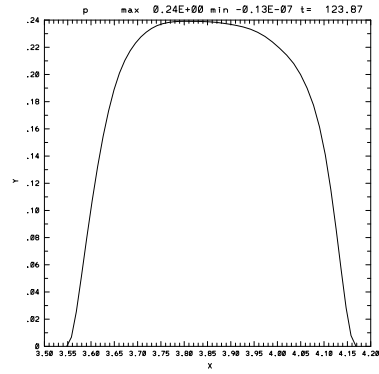
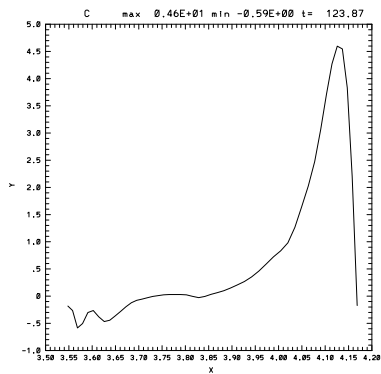
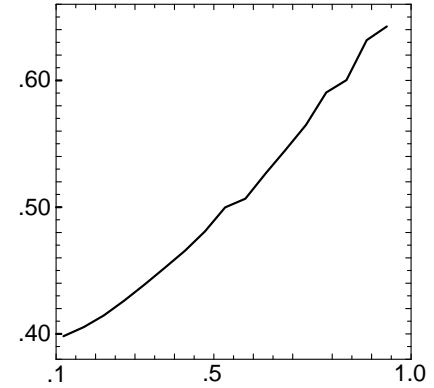
p



$v_{*e\theta}$

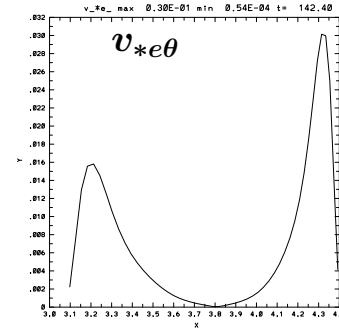
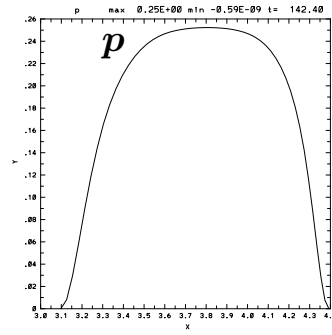
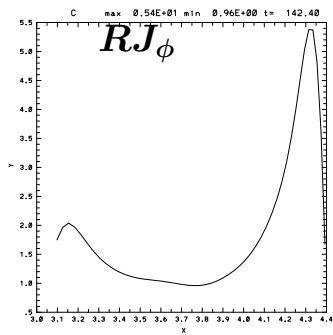
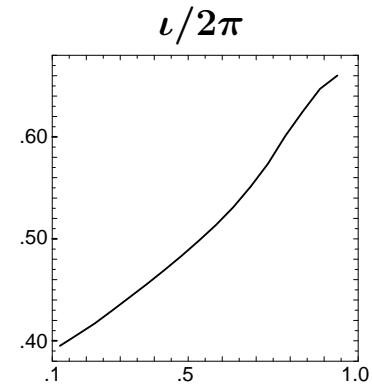
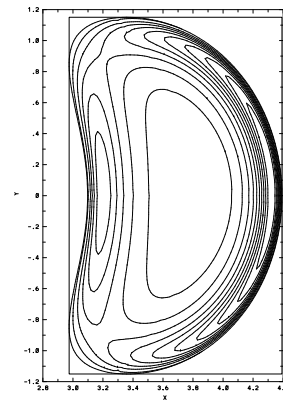
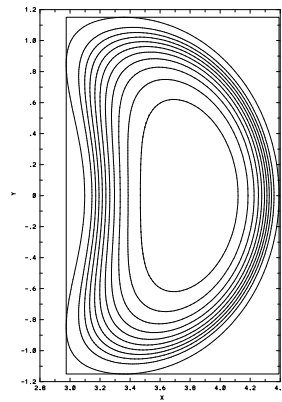
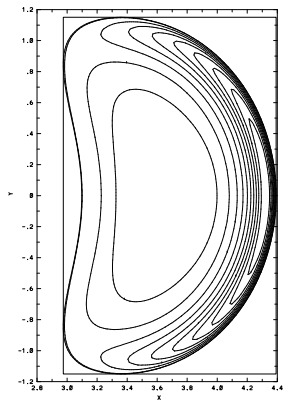


$\iota/2\pi$



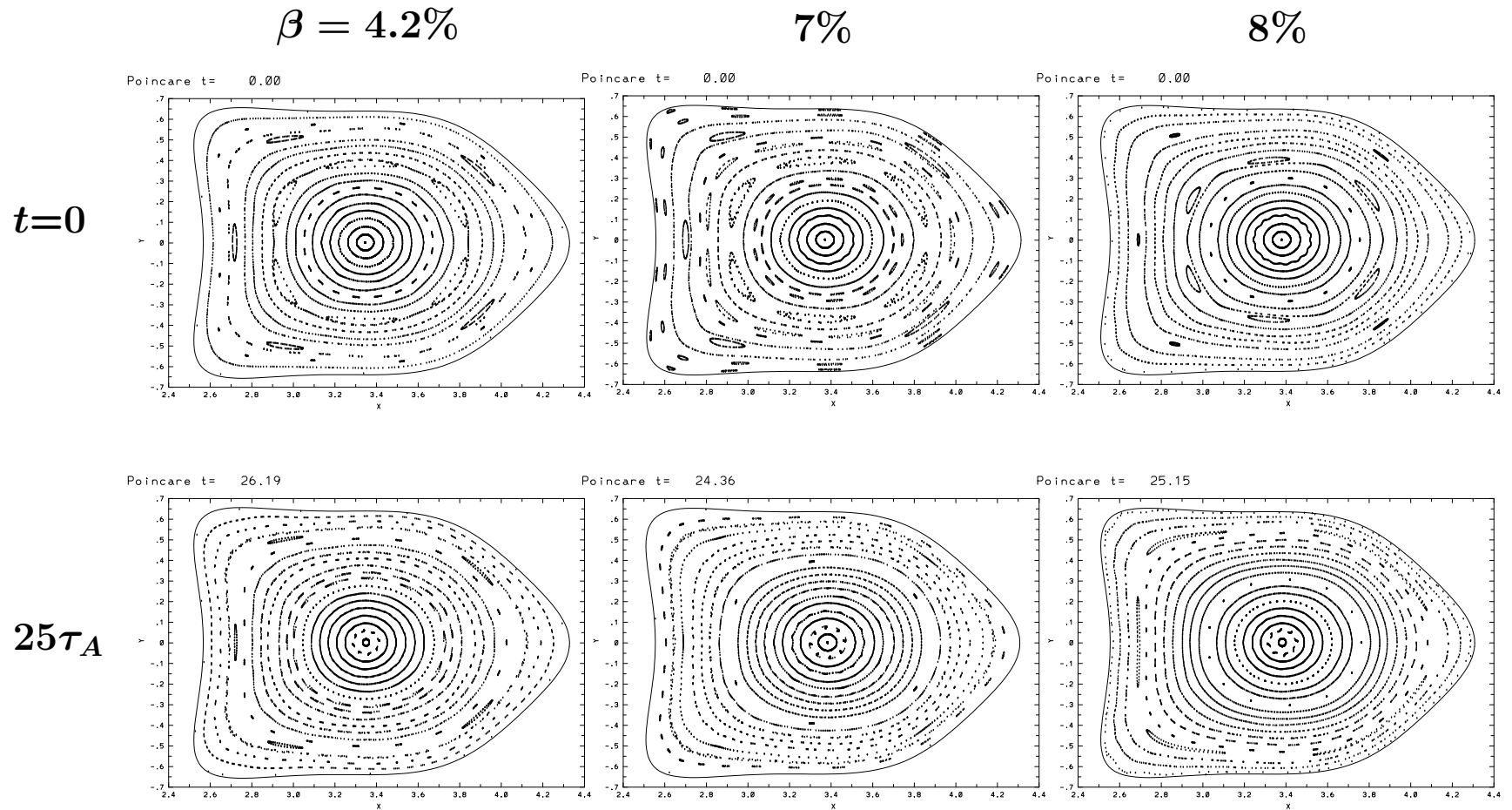
$$v_{*e} \equiv \nabla p_e \times \mathbf{B} / (enB^2)$$

- Equivalent axisymmetric equilibrium at 7% beta was calculated using same pressure and q profiles.



Stellarator:

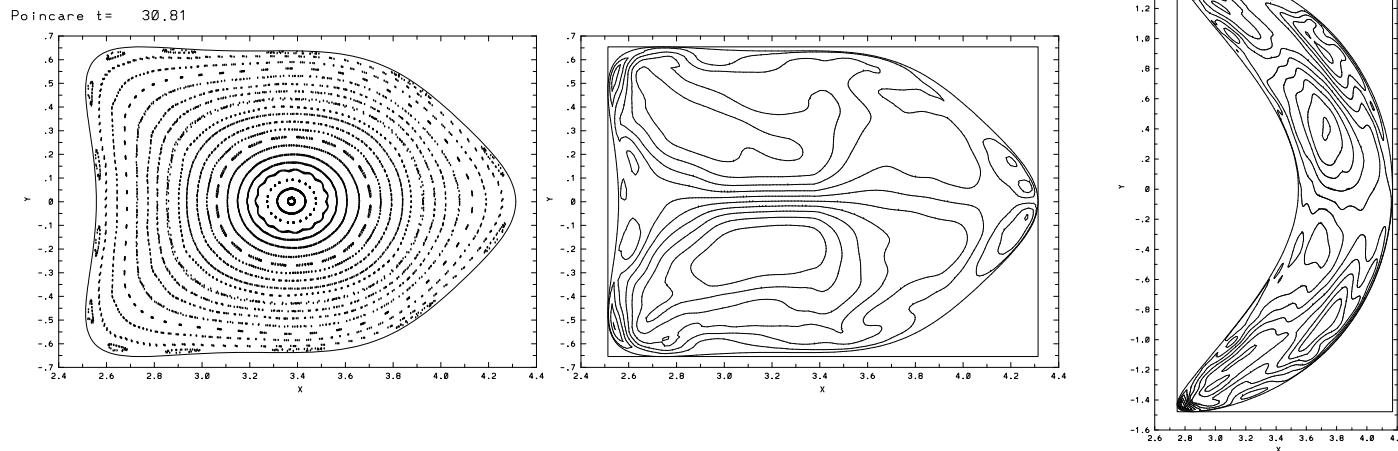
MHD resistive relaxation reduces the magnetic islands present in the initial VMEC ideal MHD equilibria.



At high beta, an MHD ballooning mode grows and rapidly causes loss of outer flux surfaces. 7% beta case.

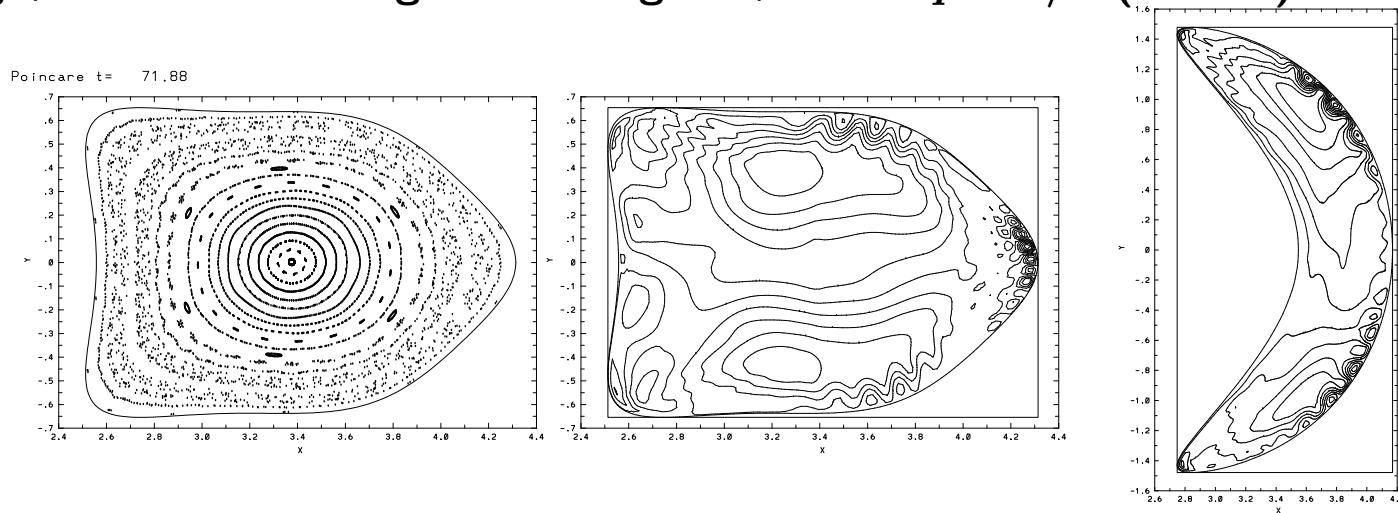
- Perturbation begins in the low magnetic shear region near the plasma edge, in the most unfavorable curvature region.

$t =$
30.8



- The mode grows in three locations. When it is large enough or extends inward enough, reconnection begins with high m, n near $q = 5/3$ ($t \simeq 62$).

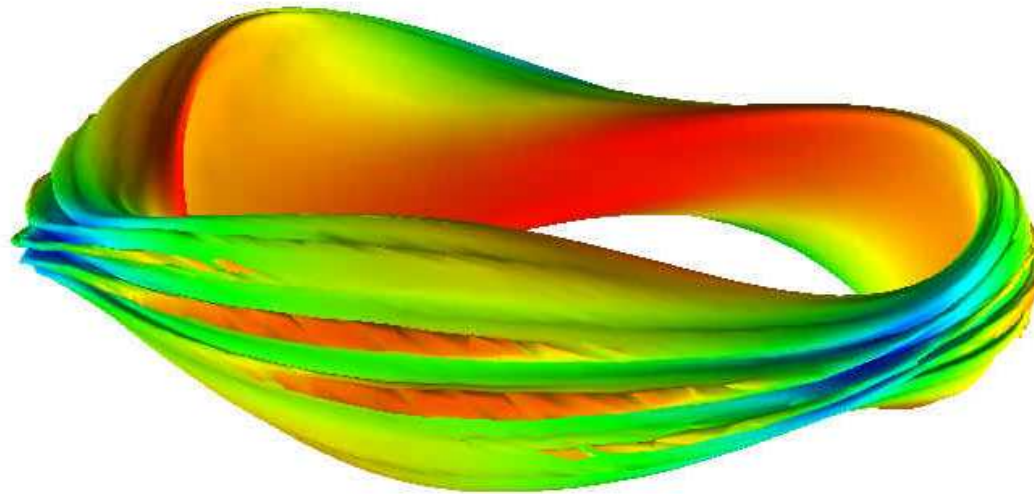
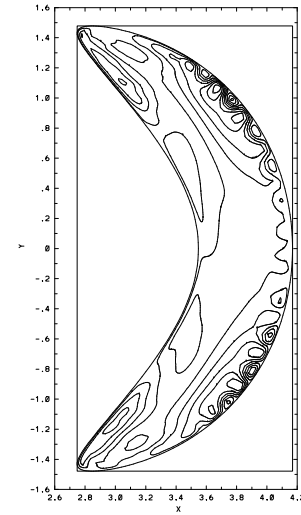
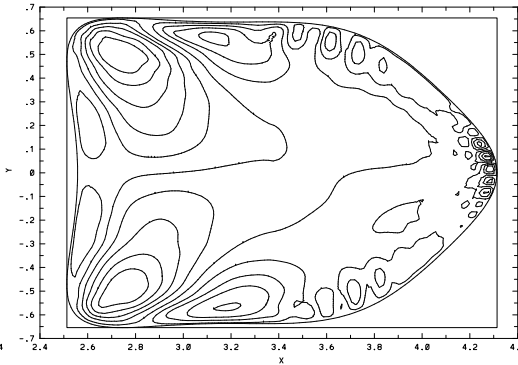
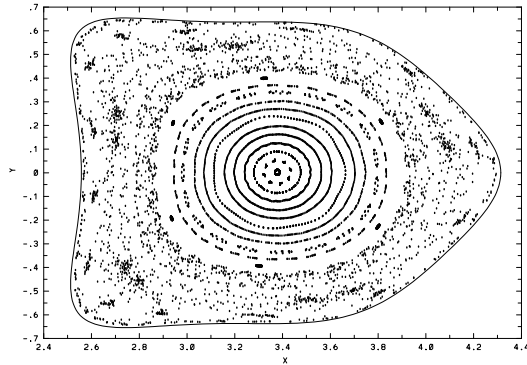
71.9



- Phase 3. Reconnection rapidly destroys the magnetic surfaces outside $q = 2$.

77.0

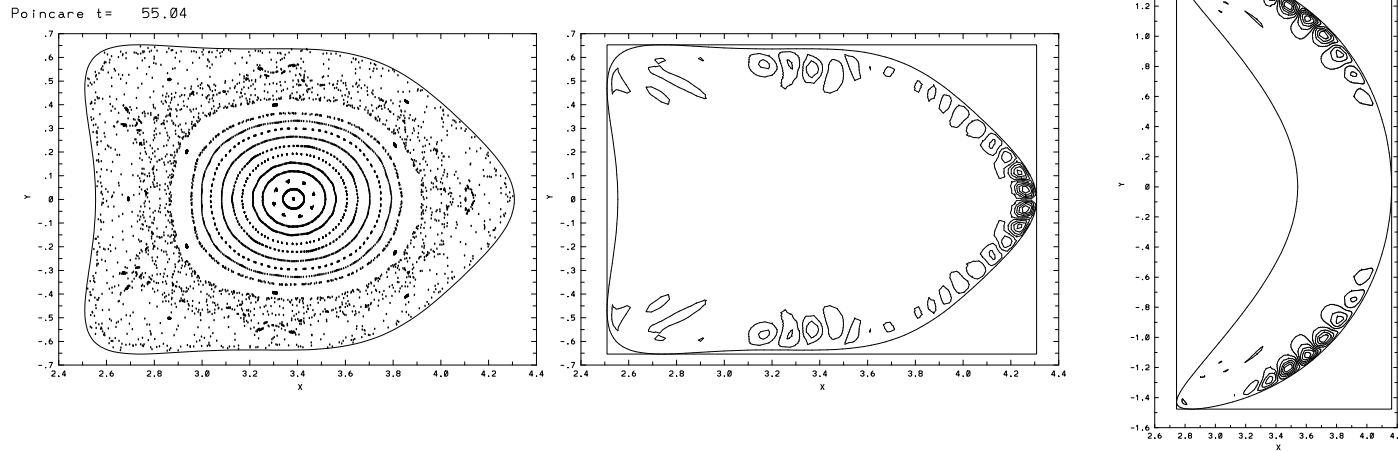
Poincare t= 77.01



Surface pressure perturbation for nonlinear ballooning mode.

MHD ballooning at 8% beta grows more rapidly and causes loss of outer flux surfaces by $t \simeq 55\tau_A$.

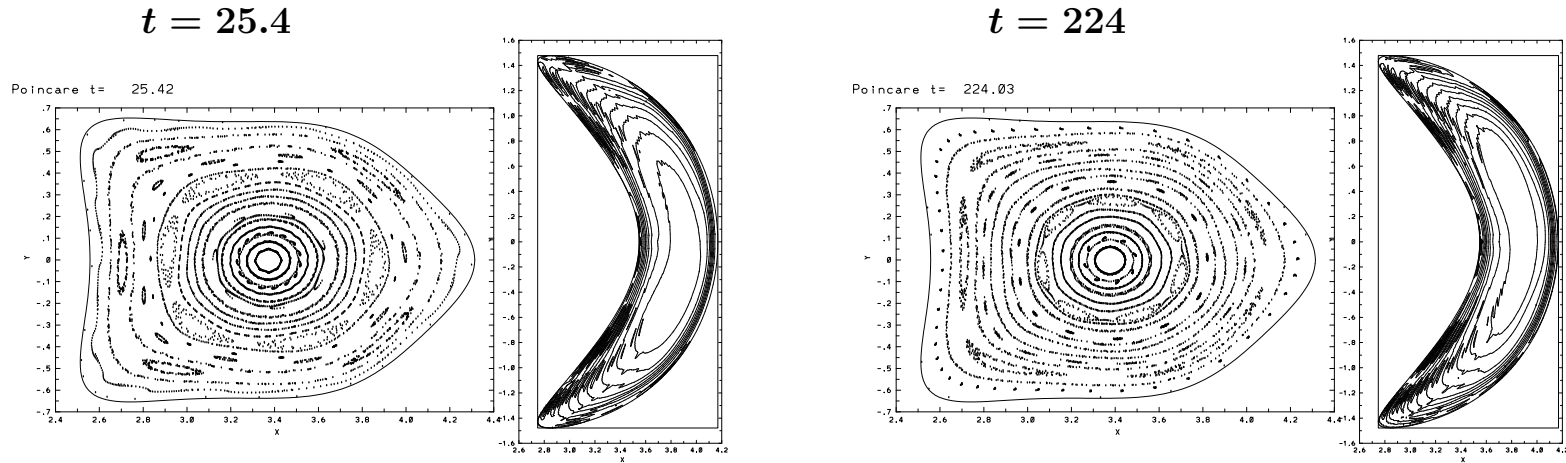
**$t =$
55.0**



- Lower spatial resolution gives somewhat different mode pattern.
- The differences seen with resolution and beta are characteristic of ideal ballooning modes.

Two-fluid effects effectively stabilize the high m,n ballooning mode at high beta, up to 8% or higher for NCSX.

Shown: $\beta = 7\%$, equilibrium $T_e = T_i$, $S = 10^5$, $H = 0.02$.



- Resistive ballooning mode is easily stabilized by FLR effects.

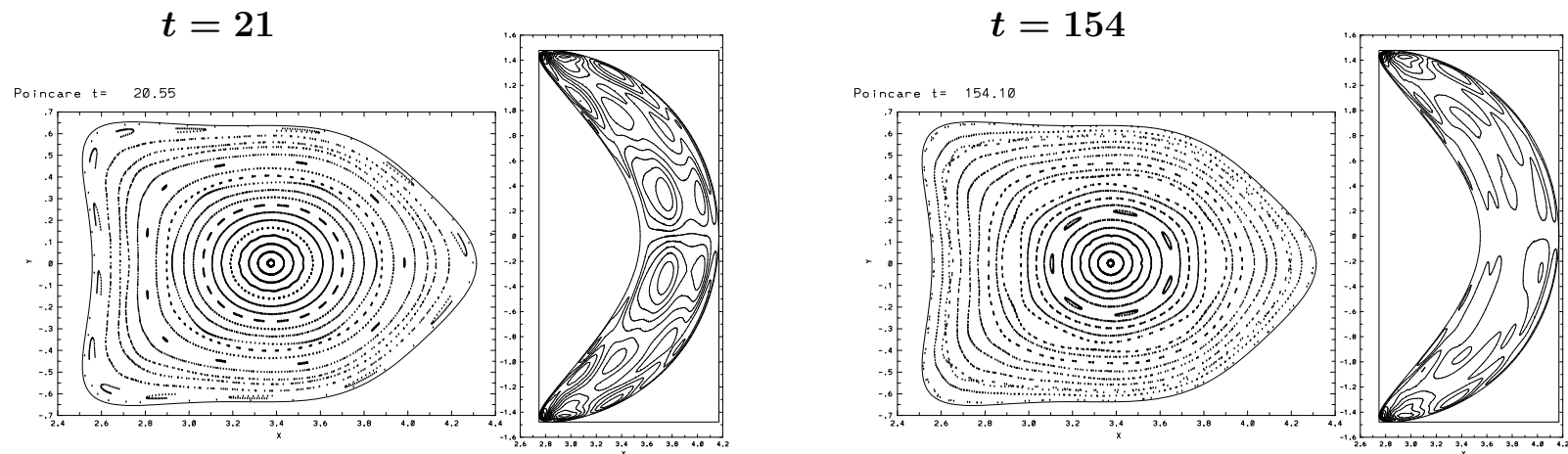
$$\omega (\omega - \omega_{*i}) (\omega - \omega_{*e}) = \eta^3 (\Delta')^4 \frac{v_A}{qR}$$

Ion FLR stabilization due to the $\omega - \omega_{*i}$ factor in the dispersion relation requires

$$\omega_{*i}/\gamma_{MHD} \gtrsim 1.$$

- Easily satisfied at realistic H ($m \simeq 30$, $H = 0.02$, $v_{*i\theta} \simeq 0.1v_A$, and $\gamma_{MHD}\tau_A \simeq 0.2$ gives $\omega_{*i}/\gamma_{MHD} \sim 15$).

- The ideal ballooning mode also has an $\omega(\omega - \omega_{*i})$ dependence due to FLR.
- **Two-fluid stabilization is robust.** It occurs at small H well below the linear FLR estimate. (Shown, $H = 2 \times 10^{-5}$ at $\beta = 7\%$ gives $\omega_{*i}/\gamma_{MHD} \simeq 0.015$, but mode is stable.)



- The observed MHD mode has many characteristics of the ideal MHD ballooning mode, which should be unstable at $\beta \geq 7\%$ at the given spatial resolution.
- The ideal ballooning mode has singular properties in 3D configurations and couples strongly to very high (infinite) n , so it should be easily stabilized by FLR and smoothing effects (Dewar and Glasser, Phys. Plasmas (1983)).

Two-fluid effects remove major MHD stability constraints on high beta stellarators and may explain observations of stellarator stability.

- Resistive MHD ballooning and interchange modes are usually theoretically unstable in stellarators, due to unfavorable curvature of the magnetic field lines.
 - They are rarely observed experimentally.
- The two-fluid simulations show that ideal MHD ballooning modes are easily stabilized by two-fluid effects, above some critical high values of m,n .
- Resistive MHD ballooning and interchange modes are also stabilized above critical m,n at realistic two-fluid values of H . (The most dangerous of these modes have high, although not infinite, mode number).
- In axisymmetric plasmas, these modes are more stable and impose less stringent theoretical limits. The equivalent axisymmetric case at 7% beta is MHD stable.

Two-Fluid Steady State: Global electrostatic potential Φ and “radial” electric field E_r exist.

- Two asymptotic limits. Large p_i/p

$$\mathbf{E} + \mathbf{v}_i \times \mathbf{B} = (1/en)\mathbf{J} \times \mathbf{B} - \nabla p_e/(en) + \eta\mathbf{J} + \dots$$

$$\mathbf{J} \times \mathbf{B} = \nabla p + \rho[(\partial\mathbf{v}_i/\partial t + \mathbf{v}_i \cdot \nabla\mathbf{v}_i)] + \nabla \cdot \Pi_{i,gv} + \mu\nabla^2\mathbf{v}_i + \dots$$

in steady state, $\mathbf{E} = -\nabla\Phi$, the perpendicular Ohm’s law yields

$$-\nabla\Phi + \mathbf{v}_i \times \mathbf{B} = \nabla p_i/(en) + \eta\mathbf{J} + \dots$$

If the ion velocity is small compared to the diamagnetic drift, $|\mathbf{v}_i \times \mathbf{B}| \ll |\nabla p_i/(en)|$, then $\nabla\Phi \simeq -\nabla p_i/en$ or $\Phi \simeq -p_i/en$ for uniform density.

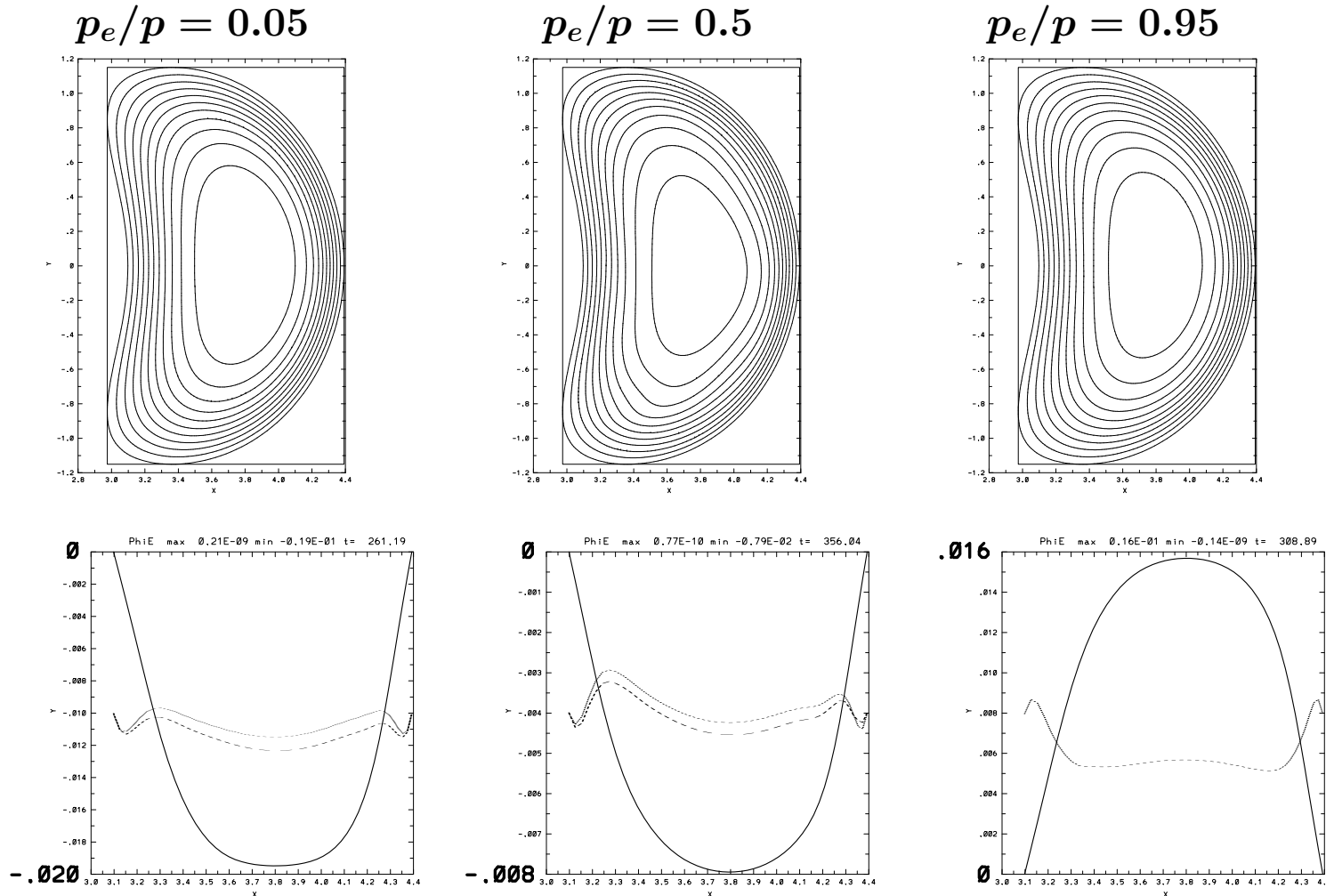
For the stellarator, the estimate can be refined by using $\times\mathbf{B}$ of Ohm’s law and comparing Φ to the \mathbf{v}_{*i} stream function U , $\mathbf{v}_{di} = \epsilon R \nabla U \times \hat{\phi} + \nabla_{\perp}\chi + v_{\phi}\hat{\phi}$, where ϕ is the toroidal angle.

- Large p_e/p

The perpendicular-to-B component yields only $-\nabla\Phi = \mathbf{v} \times \mathbf{B}$, $\mathbf{v}_i = \mathbf{v} + \mathbf{v}_{*i} \simeq \mathbf{v}$.

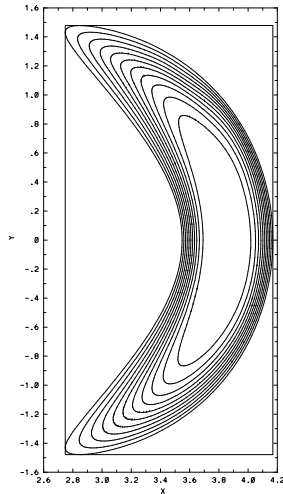
The parallel component yields $-\nabla_{\parallel}\Phi = -\nabla_{\parallel}p_e/en + \dots$, for small $\eta_{\parallel}\mathbf{J}_{\parallel}$, or $\Phi \simeq p_e/en + f(\psi)$. For small f , this has opposite sign to the large p_i limit.

- In axisymmetry, Φ has a smooth, centrally peaked shape. It fits the asymptotic limits $\Phi \simeq -p_i/en$ at small $p_e/p \lesssim 0.5$ and $\Phi \simeq +p_e/en$ at large $p_e/p \sim 1$ (dashes show differences, offset to half-height).

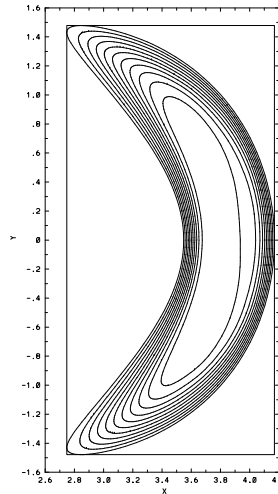


- In the stellarator, the potential Φ fits the small p_e/p asymptotic limit reasonably well (U_{di} , dashes, $-p_i/en$ dots), but diverges at higher p_e/p .
- E_r has similar magnitude to neoclassical prediction for NCSX at $p_e/p = 0.5$.

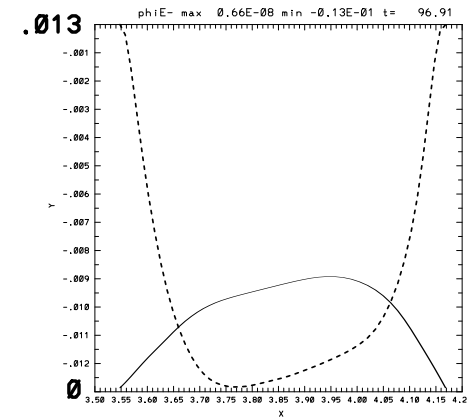
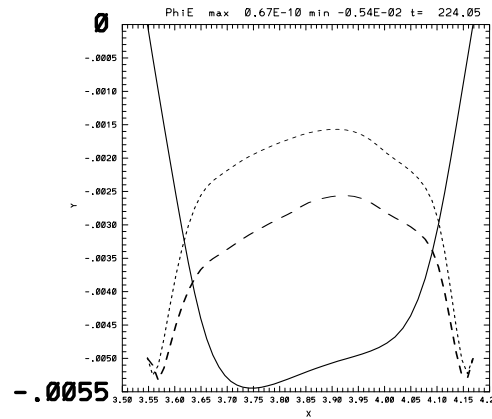
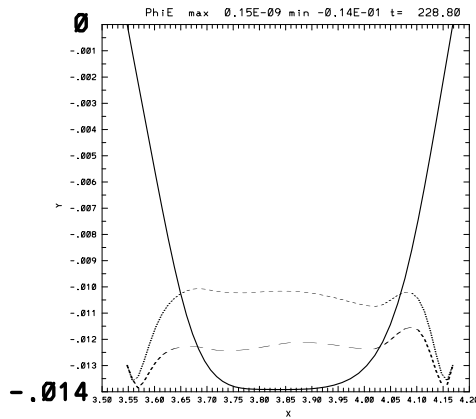
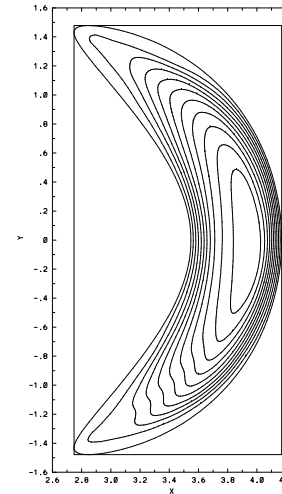
$p_e/p = 0.05$



$p_e/p = 0.5$



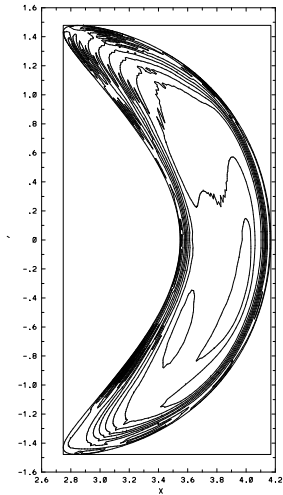
$p_e/p = 0.95$



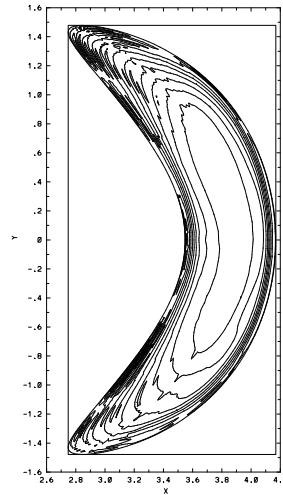
A small ion poloidal flow is set up in the stellarator.

- Stream function in the strong- ∇p region near the edge is similar for all p_e/p .

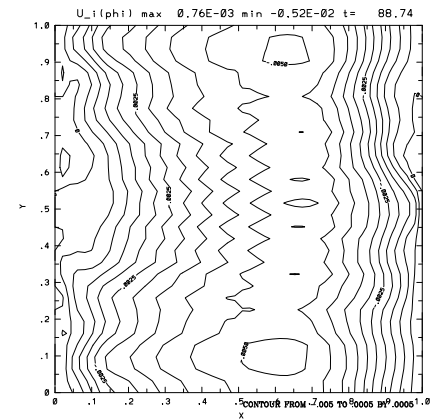
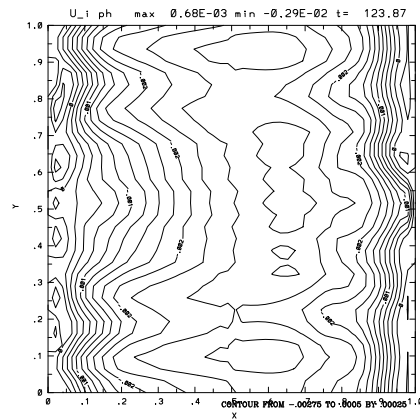
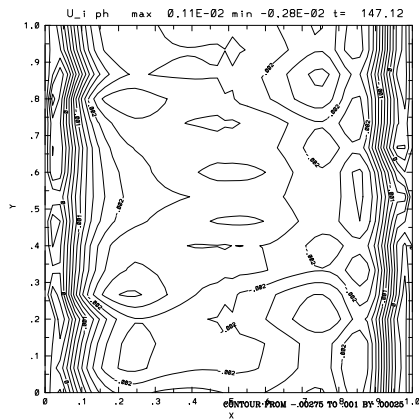
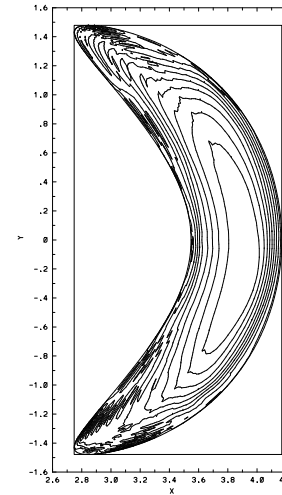
$p_e/p = 0.05$



$p_e/p = 0.5$



$p_e/p = 0.95$



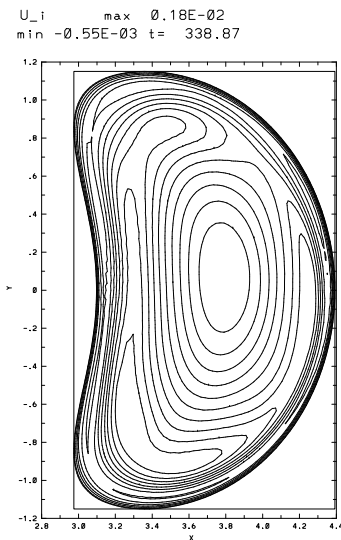
- Ion flow depends on the details of momentum balance and two-fluid model.
- In axisymmetry, the flow is different because toroidal flow is constrained by canonical momentum conservation.

For initial $v_{i\theta} = v_{i\phi} = 0$,

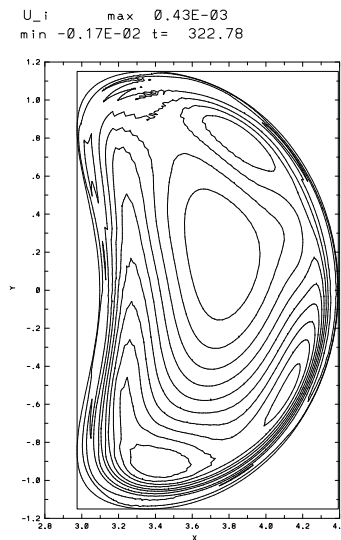
Small and moderate p_e/p have ω_{*e} -direction flow in center, reversed near edge.

Large p_e/p has centrally peaked ω_{*i} -direction flow, almost $v_{*\theta}$ from total p .

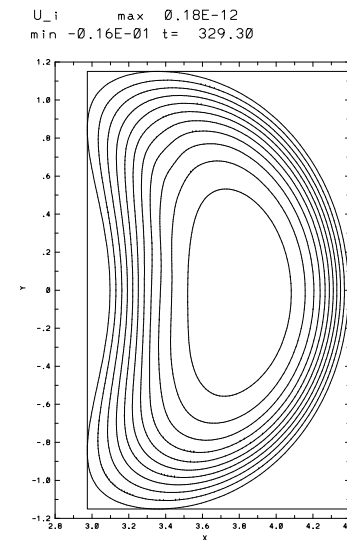
$$p_e/p = 0.05$$



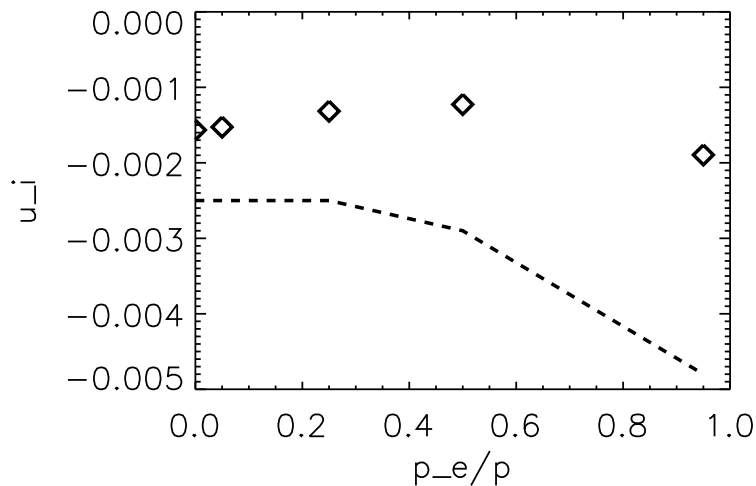
$$p_e/p = 0.5$$



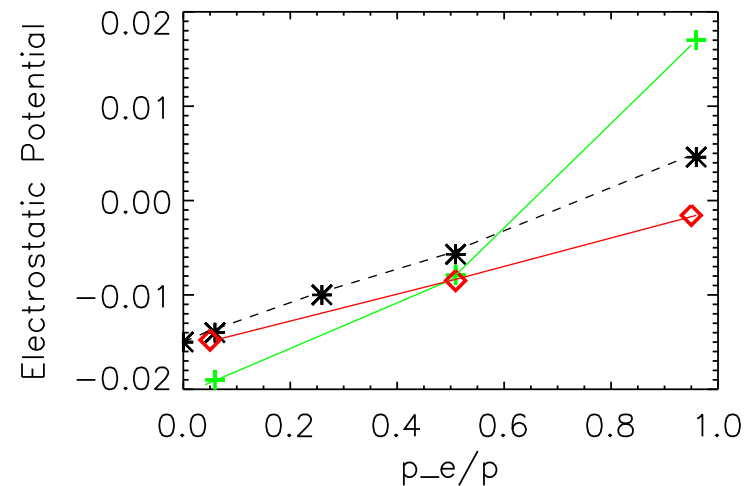
$$p_e/p = 0.95$$



- In ion regime where p_i/p is significant, Φ roughly cancels the ion diamagnetic drift $v_{*i\theta}$ and keeps the ion poloidal flow small, $|v_{i\theta}| < |v_{*i\theta}|/2$.
- At large $p_e/p \simeq 1$, the potential and field reverse sign to $E_r > 0$.
 - In the stellarator, Φ maintains a similar value of the ion flow $v_{i\theta}$ (actually, stream function U_i) in the strong ∇p region.
 - Neoclassical parallel stresses also predict E_r reversal at low collisionality (high T_e). Different physics!
- Setting $\nabla_{\parallel} p_e = 0$ in Ohm's law prevents E_r reversal in two-fluids.



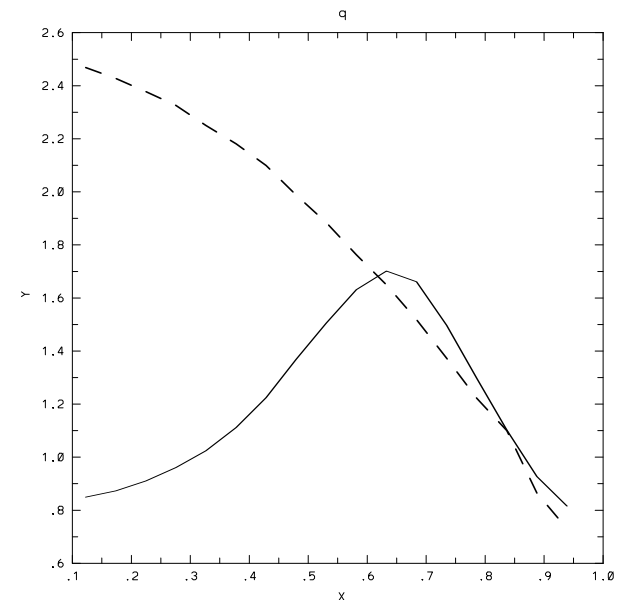
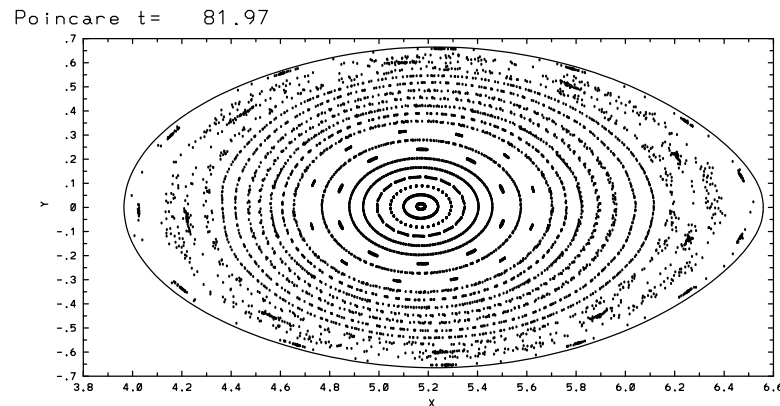
(Dashes) $r = 0$
 \diamond $r/a \simeq 0.8$



* Stellarator
 \diamond Stellarator, $\nabla_{\parallel} p_e/en \equiv 0$
 $+$ Axisymmetric

In non-axisymmetry, two-fluid magnetic flux surfaces can expand or contract in minor radius relative to MHD.

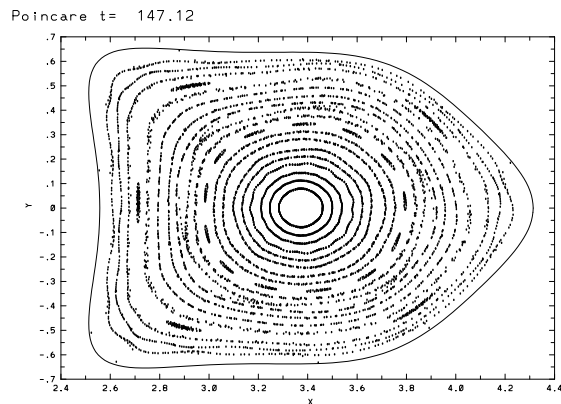
- Finite $\nabla_{\parallel} p_e / en$ and $\nabla_{\parallel} \Phi$ in Ohm's law allows $\partial\psi_{\parallel} / \partial t$. Axisymmetry eliminates the shift.
- Expansion increases with increasing two-fluid parameter H .
- For NCSX with fixed plasma boundary, expansion is seen in the central region with low equilibrium ∇p , in the fat cross section. Island growth time scale, slower than quasi-steady Φ or flow.
- For LHD, central q drops (net currentless plasma, period $l = 10$).



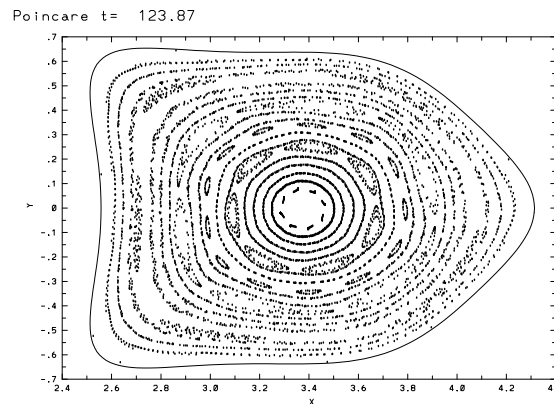
Two-fluid magnetic reconnection may set the intrinsic limit on beta in stellarators.

- Nonlinear magnetic reconnection rates at low-order rational surfaces are enhanced by increasing electron pressure, due to $\nabla_{\parallel} p_e / en$ in Ohm's law.

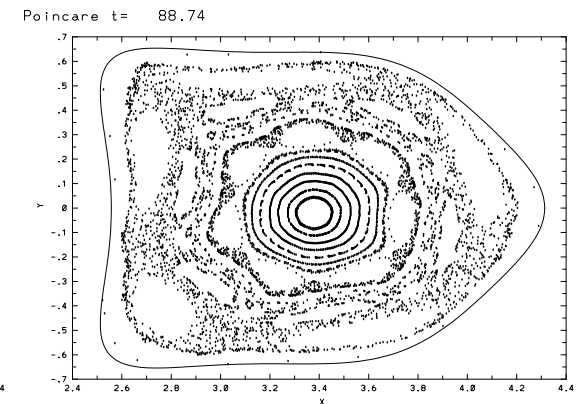
$$p_e/p = 0.05$$



$$p_e/p = 0.5$$



$$p_e/p = 0.95$$

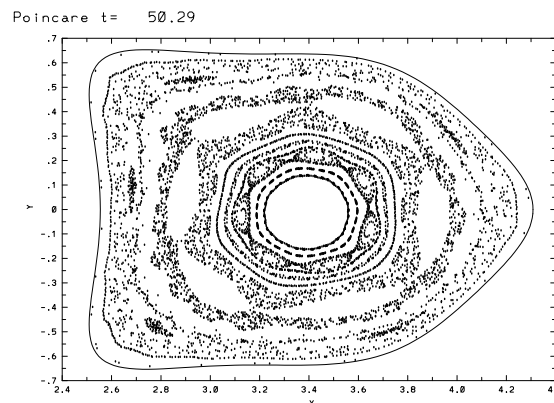


- Two-fluid reconnection rates increase strongly with beta at high beta.

$$\beta = 8\%$$

$$p_e/p = 0.5$$

$$t = 50.3$$



Magnetic island growth rates and final size correlate with the relative magnitude of $\nabla_{\parallel} p_e / (en)$.

- NCSX at 7% beta has large $|\nabla_{\parallel} p_e / (en)| \gtrsim |\eta_{\parallel} J_{\parallel}|$, despite

Large resistivity ($S = 10^5$ versus actual 10^7-10^8)

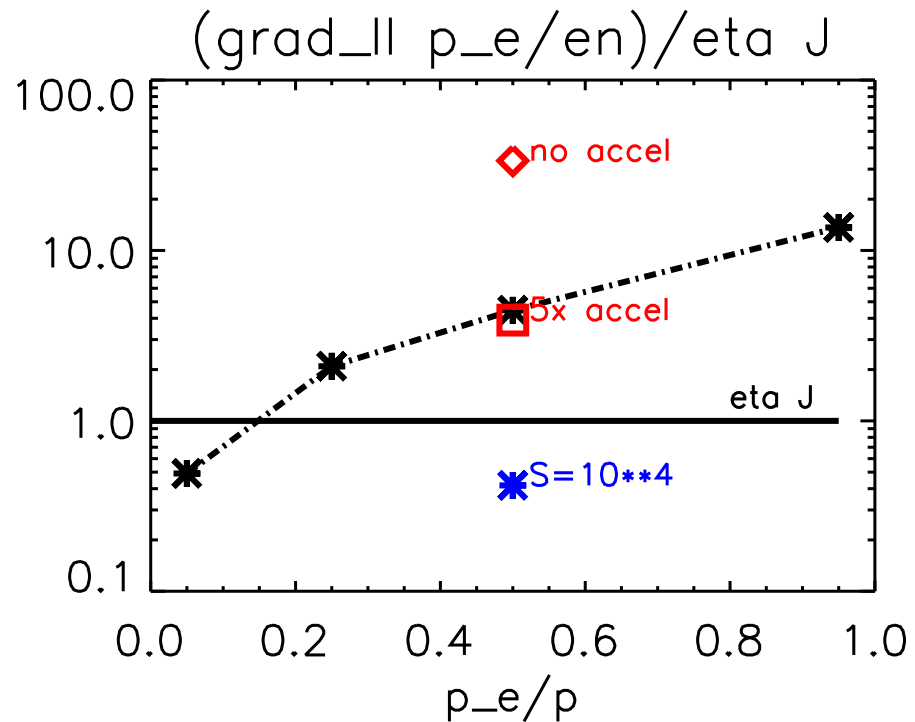
The parallel gradient $\nabla_{\parallel} p_e$ is significantly reduced by accelerated equilibration of p_e (T_e) along B.

- Ratio of maximum magnitudes over cross section.

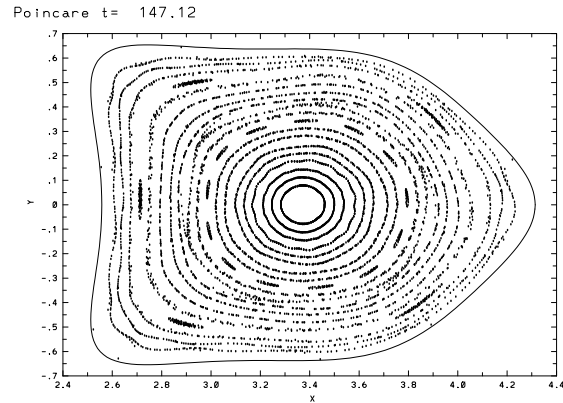
* Reference cases

Red Rate of parallel thermal equilibration $\uparrow\downarrow$

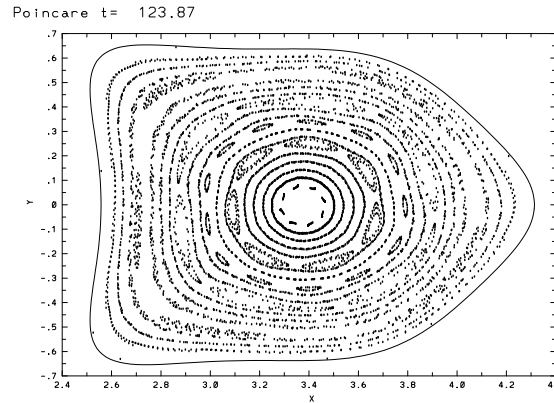
Blue Higher η



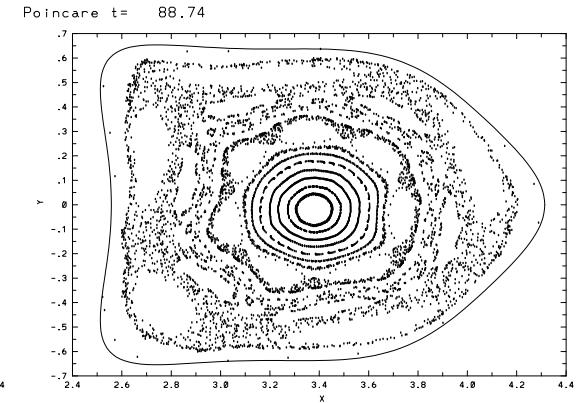
$p_e/p = 0.05$
 $S = 10^5$, Ref. $\nabla_{\parallel} p_e$ accel.



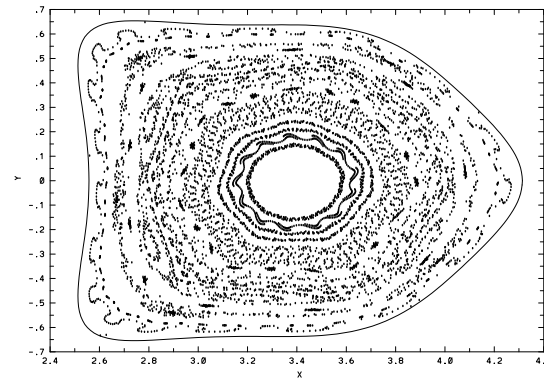
$p_e/p = 0.5$



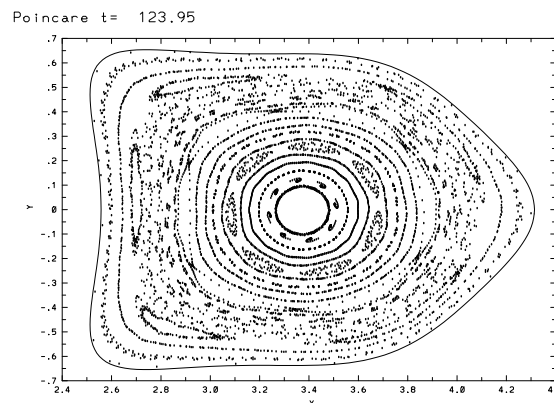
$p_e/p = 0.95$



$S = 10^5$
No \parallel acceleration
Closer to $\partial n / \partial t \neq 0$ case?



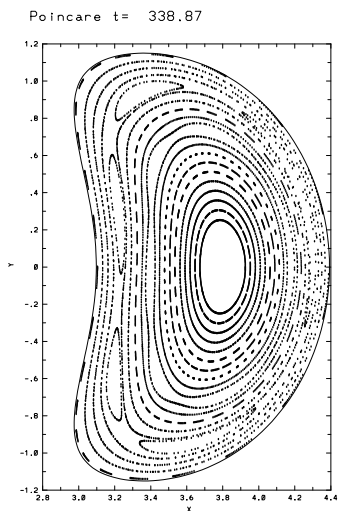
$S = 10^4$
Reference \parallel accel.



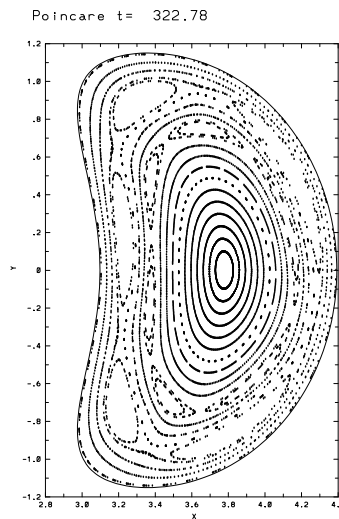
Islands grow differently in axisymmetry.

- No initial islands in axisymmetric ideal MHD equilibrium.
- Slow resistive growth until a certain critical size, then growth accelerates.
 p_e/p ratio and $\nabla_{\parallel} p_e$ equilibration rate have little effect during the first $200\tau_A$.
- After growth accelerates, island size depends on p_e/p differently than in stellarator. The 5/3, 6/3 islands grow fastest at $p_e/p = 0.5$, while high $p_e/p = 0.95$ has more higher m (shown $t \simeq 330$, $t = 376$ for $p_e/p = 0.5$).

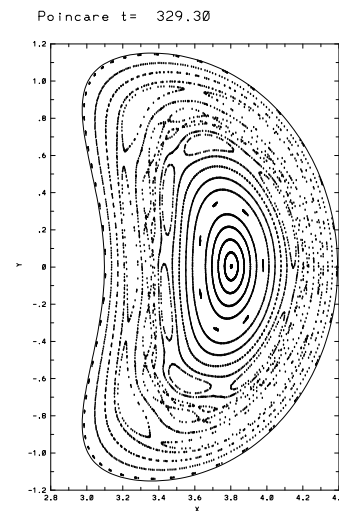
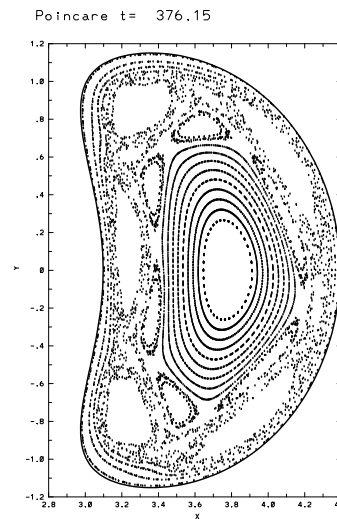
$p_e/p = 0.05$



$p_e/p = 0.50$



$p_e/p = 0.95$



- In a tokamak with normal magnetic shear, $\nabla_{\parallel} p_e / (en)$ in Ohm's law also increases nonlinear magnetic reconnection rates and saturated island sizes. Turning on the term from MHD increases the nonlinear reconnection rate and island size. Turning off the term reduces the island to the original size.
- Time evolution of 2/1 island width in a TFTR supershot-like tokamak $p_e/p = 0.5$ with MH3D-T. (Steep pressure profiles \rightarrow strong effect.)

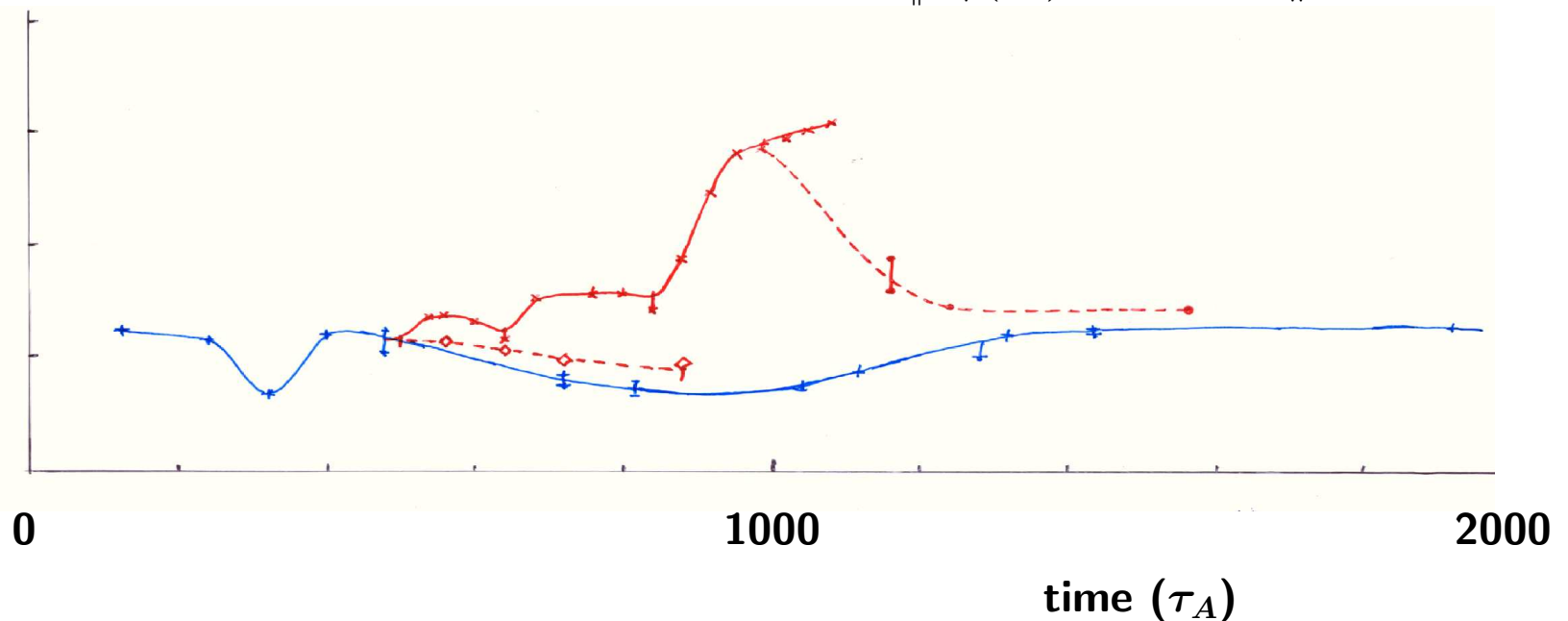
blue MHD island (saturates)

red x $\nabla_{\parallel} p_e / (en)$ on at $t = 440$

red • $\nabla_{\parallel} p_e / (en)$ turned off at $t = 980$

red \diamond $\nabla_{\parallel} p_e / (en)$ on, but fast \parallel equilibration.

Island Width



Stellarators may have an intrinsic “soft” beta limit due to deteriorating plasma confinement rather than catastrophic instability.

- The fastest growing MHD modes are stabilized by two-fluid effects.
- Magnetic reconnection at low-order interior rational surfaces increases with increasing β_e .
 - When islands become large enough, plasma confinement deteriorates to the point where applying more plasma heating will no longer raise β .
 - This behavior has been observed on W7-AS.
- **Hot-ion stellarators may have better intrinsic confinement**, since $\nabla_{\parallel} p_e$ depends on p_e/p .
- The reconnection behavior is a consequence of the helical geometry effects on magnetic island formation and on driving finite $\nabla_{\parallel} p_e$, so a soft beta limit is less important in axisymmetric configurations.

Nonlinear island growth does not follow theoretical estimates for two-fluid effects on dW/dt .

$$\frac{dW}{dt} = \frac{\eta}{(1 + \mu/\eta)^{1/2}} \left(\Delta' + \kappa \frac{\beta L_s^2}{W L_n} + g \omega' (\omega' - \omega_{*i}) \frac{L_s^2}{W^3 k^2 v_A^2} \right)$$

Term 1 = Magnetic energy (Rutherford, 1973)

Term 2 = Nonlinear interchange (Kotschenreuther, et al., 1985)

Term 3 = Polarization current effects (two-fluid, $T_i \simeq 0$) ($g > 0$, Connor, et al., 2001)

5/3 island in stellarator at 7% beta

p_e/p	ω	ω_{*i}	ω_{pl}	ω'	$\omega'(\omega' - \omega_{*i})$	$\omega(\omega - \omega_{*i})$	$ \nabla_{\parallel} p_e / (en) $
0.05	0	-1.128	-0.380	-0.749	-0.284	0	5.6×10^{-6}
0.50	0	-0.594	-0.253	-0.340	-0.0862	0	4.8×10^{-5}
0.95	0	-0.063	-0.243	+0.181	+0.0439	0	1.2×10^{-4}
0.50^c	0	-0.612	-0.351	-0.260	-0.0915	0	5.4×10^{-4}

^c No accelerated parallel thermal equilibration.

5/3 island in equivalent axisymmetric configuration

p_e/p	ω	ω_{*i}	ω_{pl}	ω'	$\omega'(\omega' - \omega_{*i})$	$\omega(\omega - \omega_{*i})$	$ \nabla_{\parallel} p_e / (en) $
0.05	-0.0114	-0.668	$\simeq 0$	-0.700	$+7.98 \times 10^{-3}$	-3.7×10^{-3}	2.0×10^{-6}
0.50	+0.0743	-0.368	$\simeq 0$	-0.294	-2.18×10^{-2}	$+1.88 \times 10^{-2}$	1.3×10^{-4}
0.95	-0.100	-0.0343	-0.186	+0.052	$+4.50 \times 10^{-3}$	$+8.3 \times 10^{-3}$	5.3×10^{-5}

- Polarization current term correctly predicts instability at large p_e/p but does not predict the observed dependence on p_e/p in either stellarator or axisymmetry.
 - Starting from healed MHD islands $t \simeq 30$ gives similar final states.
- Theories consider the reference frame $E_r = 0$, but neglect the two-fluid global steady state, where $\Phi \simeq \Phi(\psi)$ in the lab (magnet) frame and plasma flow may exist.
- Explicit dependence on $\nabla_{\parallel} p_e / (en)$ is difficult to calculate.
Pressure or temperature is not well flattened over a growing island.

CONCLUSIONS

- The first study of nonlinear two-fluid quasi-steady states in a stellarator compared to equivalent axisymmetric configurations.
Different assumptions from existing analytical theories.
- Two-fluid beta limits are significantly different from MHD for stellarators, less so for axisymmetric plasmas. They may explain several stellarator puzzles.
- High- m, n MHD instabilities are easily stabilized by FLR and other smoothing effects for realistic two-fluid values.
- Enhanced two-fluid magnetic reconnection: Stellarators may have an intrinsic “soft” beta limit due to poor plasma confinement in the presence of large two-fluid magnetic islands, which grow with β_e .
- Two-fluid global steady state conditions on Φ, E_r, v_i .
 - Two-fluid E_r behaves like neoclassical field without the $\nabla \cdot \Pi_{\parallel}$ stresses — sign reversal at large p_e/p and similar magnitude.
 - Stellarator flux (q) surfaces may expand/contract in minor radius from MHD equilibrium.
- Importance of $\nabla_{\parallel} p_e / (en)$ in Ohm’s law. Other parallel terms?